Mesoporous Silica-Reinforced Polymer Nanocomposites

Xiangling Ji,[†] J. Eric Hampsey,[†] Qingyuan Hu,[†]
Jibao He,[‡] Zhengzhong Yang,*[,§] and Yunfeng Lu*[,†]

Department of Chemical Engineering and Coordinated Instrumentation Facility, Tulane University, New Orleans, Louisiana 70118, and State Key Laboratory of Polymer Physics and Chemistry, Center for Molecular Science, Institute of Chemistry, The Chinese Academy of Sciences, Beijing 100080, China

Received April 16, 2003. Revised Manuscript Received June 22, 2003

This research reports the use of organic-modified mesoporous silica particles as fillers to form organic/inorganic nanocomposites with improved thermal and mechanical properties. The particle fillers were synthesized by co-assembly of surfactant and silicate species prepared by hydrolysis and condensation reactions of tetraethoxysilane (TEOS) and (3-trimethoxysilyl)propyl methacrylate (TMSPMA) through an aerosol process. Selective surfactant removal resulted in mesoporous particles with high surface areas and with covalently bound propyl methacrylate ligands on the pore surface as indicated by XRD, TEM, N_2 adsorption−desorption, FTIR, ^{13}C NMR, ^{29}Si NMR, and other techniques. Infiltration and subsequent in situ polymerization of (3-trimethoxysilyl)propyl methacrylate within and among the mesoporous silica particles result in nanocomposites with improved mechanical and thermal properties. Mechanical testing shows a significant increase in tensile strength, modulus, and toughness of the nanocomposites with little sacrifice on the elongation relative to the bulk poly((3-trimethoxysilyl)propyl methacrylate). DSC and SEM results indicate that chemical bonding and strong interactions between the polymer and filler, confined segmental motion of the polymer chains within the mesoporous channels, and the use of the silica particles as pseudo-cross-linking points may contribute to the improved mechanical properties.

Introduction

Silica/polymer nanocomposites are a promising new class of materials that have many possible applications in aerospace materials, structural materials, electronics, sensors, and other areas.[1−29] Three main synthesis approaches have been developed to produce the silica/polymer nanocomposites. The first approach involves mixing polymers with silica particles or silica precursors directly. For example, silica composites of poly(methyl methacrylate), poly(ethylene glycol), and polyurethane have been prepared by mixing these polymers with silica colloids in solution or silica precursors (e.g., tetraalkoxysilanes) that hydrolyze and condense to form silica within the polymer matrix.[1−4] The second synthesis approach usually involves direct mixing of the polymer monomers with silica particles followed by polymeriza-

* To whom correspondence should be addressed.
[†] Department of Chemical Engineering.
[‡] Coordinated Instrumentation Facility.
[§] The Chinese Academy of Sciences.

(1) Landry, C. J. T.; Coltrain, B. K.; Brady, B. K. *Polymer* **1992**, *33*, 1486−1495.
(2) Landry, C. J. T.; Coltrain, B. K.; Wesson, J. A.; Zumbulyadis, N.; Lippert, J. L. *Polymer* **1992**, *33*, 1496−1506.
(3) Laridjan, M.; Lafontaine, E.; Bayle, J. P.; Judeinstein, P. *J. Mater. Sci.* **1999**, *34*, 5945−5953.
(4) Petrovic, Z. S.; Javni, I.; Waddon, A.; Banhegyi, G. *J. Appl. Polym. Sci.* **2000**, *76*, 133−151.
(5) Frisch, H. L.; Mark, J. E. *Chem. Mater.* **1996**, *8*, 1735−1738.
(6) Pu, Z.; Mark, J. E.; Jethmalani, J. M.; Ford, W. T. *Chem. Mater.* **1997**, *9*, 2442−2447.
(7) Moller, K.; Bein, T.; Fischer, R. X. *Chem. Mater.* **1998**, *10*, 1841−1852.
(8) Yang, F.; Ou, Y.; Yu, Z. *J. Appl. Polym. Sci.* **1998**, *69*, 355−361.
(9) Ou, Y.; Yang, F.; Yu, Z. *J. Polym. Sci., Part B: Polym. Phys.* **1998**, *36*, 789−795.
(10) Kageyama, K.; Tamazawa, J.; Aida, T. *Science* **1999**, *285*, 2113−2115.
(11) Hajji, P.; David, L.; Gerard, J. F.; Pascault, J. P.; Vigier, G. *J. Polym. Sci.* **1999**, *37*, 3172−3187.
(12) Li, Y.; Yu, J.; Guo, Z. *J. Appl. Polym. Sci.* **2002**, *84*, 827−834.
(13) Lu, G. T.; Huang, Y. *J. Mater. Sci.* **2002**, *37*, 2305−2309.
(14) Rong, J.; Yang, Z. *Macromol. Mater. Eng.* **2002**, *287*, 11−15.
(15) Zhou, Q.; Wang, S.; Fan, X.; Advincula, R.; Mays, J. *Langmuir* **2002**, *18*, 3324−3331.
(16) Terrill, N. J.; Crowley, T.; Gill, M.; Armes, S. P. *Langmuir* **1993**, *9*, 2093−2096.
(17) Stejskal, J.; Kratochvil, P.; Armes, S. P.; Lascelles, S. F.; Riede, A.; Helmstedt, M.; Prokes, J.; Krivka, I. *Macromolecules* **1996**, *29*, 6814−6819.
(18) Lascelles, S. F.; McCarthy, G. P.; Butterworth: M. D.; Armes, S. P. *Colloid Polym. Sci.* **1998**, *276*, 893−902.
(19) Goller, M. I.; Barthet, C.; McCarthy, G. P.; Corradi, R.; Newby, B. P.; Wilson, S. A.; Armes, S. P.; Luk, S. Y. *Colloid Polym. Sci.* **1998**, *276*, 1010−1018.
(20) Ray, S. S.; Biswas, M. *Mater. Res. Bull.* **1998**, *33*, 533−538.
(21) Barthet, C.; Hickey, A. J.; Cairns, D. B.; Armes, S. P. *Adv. Mater.* **1999**, *11*, 408−410.
(22) Percy, M. J.; Barthet, C.; Lobb, J. C.; Khan, M. A.; Lascelles, S. F.; Vamvakaki, M.; Armes, S. P. *Langmuir* **2000**, *16*, 6913−6920.
(23) Luna-Xavier, J.-L.; Bourgeat-Lami, E.; Guyot, A. *Colloid Polym. Sci.* **2001**, *279*, 947−958.
(24) Amalvy, J. I.; Percy, M. J.; Armes, S. P.; Wiese, H. *Langmuir* **2001**, *17*, 4770−4778.
(25) Percy, M. J.; Armes, S. P. *Langmuir* **2002**, *18*, 4562−4565.
(26) Luna-Xavier, J.-L.; Guyot, A.; Bourgeat-Lami, E. *J. Colloid Interface Sci.* **2002**, *250*, 82−92.
(27) Kawashima, D.; Aihara, T.; Kobayashi, Y.; Kyotani, T.; Tomita, A. *Chem. Mater.* **2000**, *12*, 3397−3401.
(28) Hsiue, G.-H.; Kuo, W.-J.; Huang, Y.-P.; Jeng, R.-J. *Polymer* **2000**, *41*, 2813−2825.
(29) Tong, X.; Tang, T.; Zhang, Q.; Feng, Z.; Huang, B. *J. Appl. Polym. Sci.* **2002**, *83*, 446−454.

10.1021/cm0300866 CCC: $25.00
Published on Web 08/27/2003

tion of the monomers.[5−26] For example, silica colloids in solution have been mixed with organic monomers such as styrene, methyl methacrylate, ethyl acrylate, and 2-hydroxyethyl methacrylate. Subsequent polymerization of these monomers led to the formation of silica nanocomposites. The third synthesis approach involves mixing both silica precursors and polymer monomers followed by simultaneous polymerization of the precursors and monomers.[11,27−29] Silica composites of polystyrene, poly(2-hydroxyethyl methacrylate), or poly(furfuryl alcohol) have been prepared using this approach.

As-synthesized silica nanocomposites usually contain dense silica particles dispersed within a polymer matrix. Generally, addition of rigid silica particles to a polymer matrix results in an increase in the strength, modulus, and thermal stability of the composite, but sacrifices toughness.[9] It has been found that strong interactions or chemical bonding between the polymer components and the inorganic fillers may provide improvement on both reinforcement and toughening. For example, nylon 6/silica nanocomposites exhibit improved impact strength, tensile strength, elongation at break, and toughness due to the strong interactions along the organic/inorganic interface.[9] The enhanced chemical bonding between silica and the polymer may also result in better thermal stability.[30]

In this research, we attempted to synthesize silica/polymer nanocomposites using mesoporous silica particles as fillers. The method of synthesizing mesoporous silica using self-assembled surfactant as templates has been well-developed since their discovery in 1992.[31] Usually, surfactant-templated mesoporous silica contains ordered (e.g., hexagonal, cubic, and lamellar pore channels), monodispersed, and controllable pore structures (pore sizes may vary from 2 to 20 nm) with surface areas higher than 1000 m^2/g. Such unique pore structures provide excellent scaffolds for the fabrication of hybrid organic−inorganic nanocomposites.[5,7,14,33−37] For example, polymerization of vinyl acetate, styrene, and methyl methacrylate has been carried out within the pore channels of the mesoporous silica.[5,7] The constrained pore geometry or strong host−guest interactions may lead to an increase or even disappearance of the glass transition temperature of the polymers.[1,6,14,35,40,41] Our previous research has developed an efficient and low-cost approach to fabricate mesoporous silica particles using a simple aerosol-assisted surfactant-assembly process.[32] In this research, we use these particles as fillers to synthesize poly((3-trimethoxysilyl)propyl methacrylate)/silica nanocomposites. The synthesis procedure involves infiltration and subsequent polymerization of the monomer (3-trimethoxysilyl)-propyl methacrylate within the mesoporous channels and among the filler particles. These nanocomposites will be then used as a model system to study the effect of mesoporous fillers on the properties of the nanocomposites.

Scheme 1. Chemical Structure of (3-Trimethoxysilyl)propyl Methacrylate (TMSPMA)

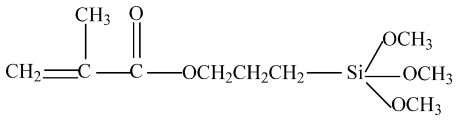

Scheme 2. Schematic Illustration for the Formation of Polymer−Mesoporous Silica Nanocomposites

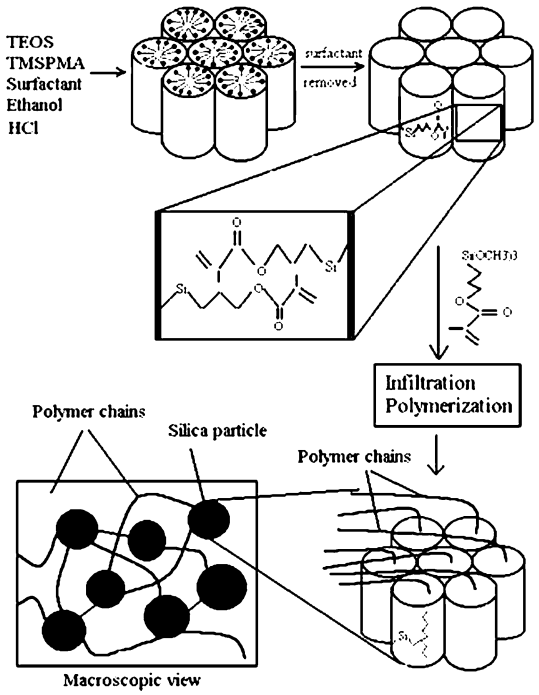

Scheme 1 shows the chemical formula of a (3-trimethoxysilyl)propyl methacrylate (TMSPMA) molecule that contains a carbon−carbon double bond (C═C) and methoxylsilane groups ($Si(OCH_3)_3$).

The former group is suitable for free radical polymerization and the latter group can form a three-dimensional silica network through hydrolysis and condensation reactions. To improve the miscibility of TMSPMA monomer with the mesoporous silica particles, we modified the mesoporous silica with TMSPMA to generate covalently bonded carbon−carbon double bonds on the pore surface of the fillers.[38] Scheme 2 shows a conceptual illustration for the formation of polymer−mesoporous silica nanocomposites. Hydrolysis and condensation of TEOS and TMSPMA in an acidic water/ethanol solvent result in sols containing organic-modified silicate species. Co-assembly of the silicate species with surfactant results in surfactant/silica nanocomposites containing the propyl methacrylate ligands. Selective removal of the surfactant leads to the formation of mesoporous silica with propyl methacrylate ligands covalently bound to the pore surface. Polymerization of the particle containing monomer results in

(30) Bershtein, V. A.; Egorova, L. M.; Yakushev, P. N.; Pissis, P.; Sysel, P.; Brozova, L. *J. Polym. Sci., Part B: Polym. Phys.* **2002**, *40*, 1056−1069.
(31) Kresge, C. T.; Leonowicz, M. E.; Roth, W. J.; Vartuli, J. C.; Beck, J. S. *Nature* **1992**, *359*, 710−712.
(32) Lu, Y.; Fan, H.; Stump, A.; Ward, T. L.; Rieker, T.; Brinker, C. J. *Nature* **1999**, *398*, 223−226.
(33) Stein, A.; Melde, B. J.; Schroden, R. C. *Adv. Mater.* **2000**, *12*, 1403−1419.
(34) Tajima, K.; Aida, T. *Chem. Commun.* **2000**, 2399−2412.
(35) Llewellyn, P. L.; Ciesla, U.; Decher, H.; Stadler, P.; Schueth, F.; Unger, K. K. *Stud. Surf. Sci. Catal.* **1994**, *84*, 2013−2020.
(36) Ng, S. M.; Ogino, S.; Aida, T.; Koyano, K. A.; Tatsumi, T. *Makromol. Chem., Rapid Commun.* **1997**, *18*, 991−996.
(37) Moller, K.; Bein, T. *Stud. Surf. Sci. Catal.* **1998**, *117*, 53−64.
(38) Ji, X.; Lu, Y., Unpublished results.

homogeneous, chemically bonded hybrid inorganic−organic composites. Since the polymerization may occur within both the pore channels and among the particles, as-synthesized composites may contain dispersed particles with polymer chains threaded within their pore channels. Compared with the conventional inorganic particle/polymer nanocomposites prepared using dense silica particles as fillers, the use of mesoporous particles as fillers may allow us to utilize these filler particles as pseudo-cross-linkers to improve the mechanical properties. Also, the larger organic/inorganic interface may significantly affect the properties of the nanocomposites.

Experimental Section

Preparation of the Mesoporous Silica Particles. Tetraethoxysilane (TEOS), (3-trimethoxysilyl)propyl methacrylate (TMSPMA), and the surfactant Brij-56 ($CH_3(CH_2)_{15}-(OCH_2-CH_2)_{10}-OH$) were purchased from Aldrich and were used directly with further purification. The detailed synthesis procedure of the mesoporous silica particles has been described elsewhere.[32,38] Briefly, the synthesis process starts with a silica sol prepared by hydrolysis and condensation reactions of TEOS and TMSPMA (TMSPMA:TEOS = 30/70 in molar ratio) in an acidic ethanol/water solvent. The surfactant Brij-56 was added to the sol and used as the pore template. Aerosol droplets generated by an atomizer were passed through a heating zone at 400 °C and collected on a filter. The surfactant was extracted from the particles using ethanol as solvent.

Synthesis of Poly(TMSPMA)−Mesoporous Silica Composites. Silica filler particles were first degassed under vacuum at 90 °C to remove water moisture and contaminants within the pores. The monomer (3-trimethoxysilyl)propyl methacrylate (TMSPMA) with 0.5 wt % 2,2-azobisisobutyronitrile (AIBN from Aldrich) as an initiator was also degassed for half an hour. The monomer and filler particles were then mixed under vacuum to produce a transparent or translucent particle/monomer solution. The mixtures were polymerized in an ultrasonic bath at 55−60 °C for 4 h. The polymerized samples were then further polymerized at 65 °C for 2 days and at 100 °C for 1 day. The resulting polymer and nanocomposites were extracted with anhydrous tetrahydrofuran, and no significant weight loss was measured after drying. For detailed spectroscopic information (FT-IR spectra) on the extent of monomer conversion, see the Supporting Information.

Characterizations. Low-angle powder X-ray diffraction patterns (XRD) were obtained with a Scintag XDS 2000 X-ray diffractometer equipped with monochromated Cu Kα radiation ($\lambda = 1.5406$ Å) in the range of $0.8° < 2\theta < 6°$. Infrared spectra of the samples were recorded on a NEXUS 670 FT-IR spectrometer (Thermo Nicolet Co.) with a resolution of 4 cm^{-1}. The solid samples were prepared with a conventional KBr pressing method. The liquid samples were measured with a KBr holder. Nitrogen adsorption−desorption isotherms at 77 K for mesoporous silica particles were obtained using a Micromeritics ASAP 2010. The specific surface area is calculated by the Brunauer−Emmett−Teller (BET) method while pore size is obtained from the Barrett−Joyner−Halenda (BJH) model. Both ^{13}C and ^{29}Si MAS solid-state NMR experiments were performed on a 400-MHz AV400 NMR spectrometer (Bruker, Switzerland). Stress−strain curves were recorded using a Model 5567 Instron tester. The samples were cut into strips with dimensions of 20.0 (L) × 2.5 (W) × 1.0 (H) mm^3, and the tensile tests were carried out on at least five strips for each specimen at room temperature with a cross-head speed of 50 mm/min. The glass transition temperature (T_g) was measured with a 2920 MDSC (TA Instruments) in the range of −60 to 250 °C under a nitrogen atmosphere at a heating rate of 20 °C/min. Thermogravimetric analysis (TGA) was performed with a 2960 SDT (TA Instruments). Approximately 10−20 mg of sample was heated from 40 to 700 °C at a heating rate of 20 °C/min under an argon atmosphere. Scanning electron microscopy (SEM) images were taken with a JSM-5410 (JEOL, Inc). The SEM samples were prepared by dispersing the silica particles directly onto carbon tape or by breaking the composites in liquid N_2. The samples were then sputtered with carbon prior to the SEM observation. Transmission electron microscopy (TEM) images were taken with a JEOL 2010 electron microscope with an accelerating voltage of 120 kV. The TEM samples were prepared by dispersing the silica particles directly onto copper grids.

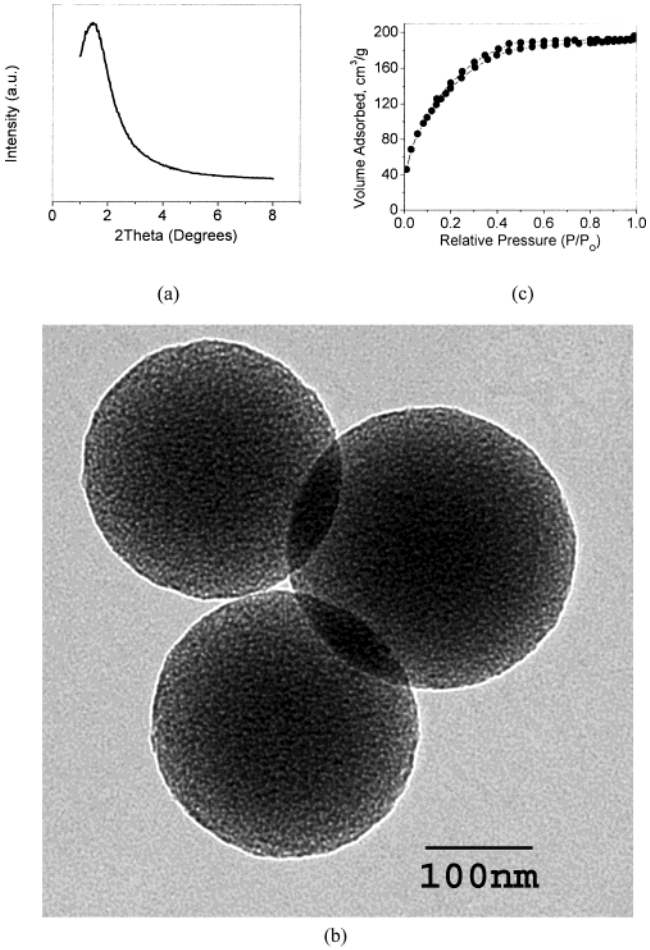

Figure 1. (a) Powder X-ray diffraction (XRD) pattern, (b) TEM image, and (c) N_2 adsorption−desorption isotherms of the TMSPMA-modified mesoporous silica particles.

Results and Discussion

1. Organically Modified Mesoporous Silica Particles. Figure 1 shows (a) an X-ray diffraction (XRD) pattern, (b) a TEM image, and (c) nitrogen adsorption−desorption isotherms of the mesoporous TMSPMA-modified particles. The XRD pattern shows a broad diffraction peak at 2θ 1.500°, corresponding to a d spacing of 59 Å. The TEM image in Figure 1b indicates wormlike pore structures with an average pore-to-pore distance of 60 Å, which is consistent with the XRD result. The nitrogen adsorption−desorption isotherms show a slight hysteresis loop. These mesoporous particles have a surface area of 577 m^2/g, an average pore size of 29.3 Å, and a pore volume of 0.38 cm^3/g.

Figure 2 shows (a) FT-IR, (b) solid-state ^{13}C NMR, and (c) ^{29}Si NMR spectra of the TMSPMA-modified particles. The FT-IR spectrum (Figure 2a) shows the C−H stretching vibration at 2971 and 2900 cm^{-1} and an intense C═O stretching vibration at 1742 cm^{-1}. The band at 1641 cm^{-1} possibly comes from both the C═C

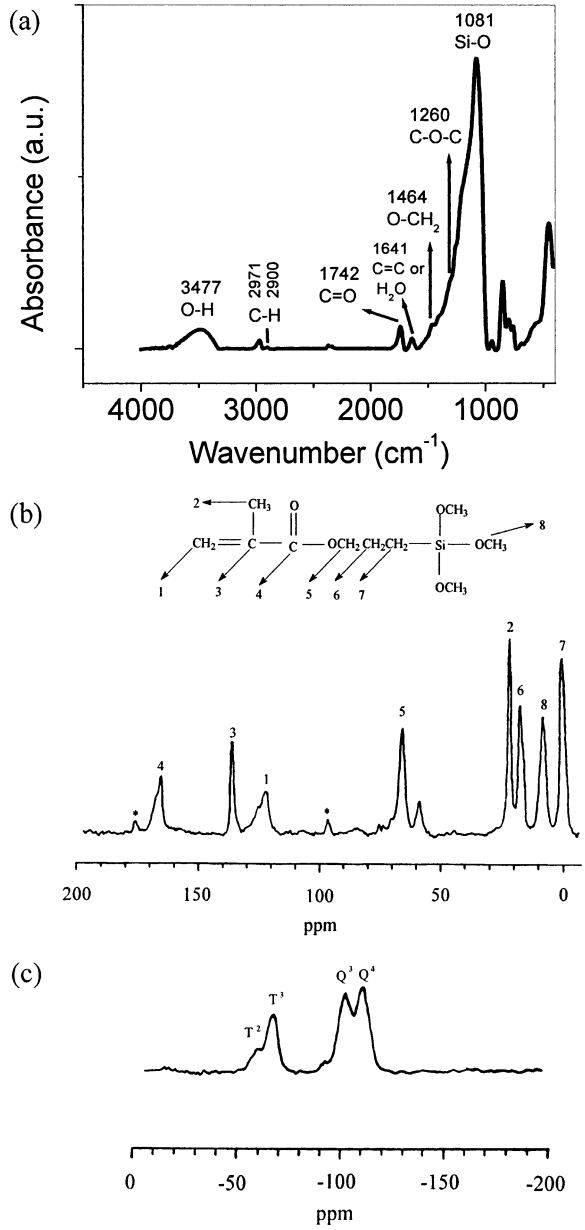

Figure 2. (a) FT-IR, (b) ^{13}C CP/MAS NMR, * spinning sidebands, and (c) ^{29}Si MAS NMR spectra of the TMSPMA-modified mesoporous silica particles.

groups and water. A broad and intense band between 3300 and 3700 cm^{-1} is associated with Si−OH groups, which can lead to adsorption of water molecules on the surface of the pore channels. The $O-CH_2$ and CH_3 vibrations have been observed at 1464 cm^{-1}, and a band at 1260 cm^{-1} is due to the C−O−C asymmetric stretching vibration. The FT-IR result confirms the formation of organic-modified mesoporous silica.

The presence of the organic functional groups within the mesoporous particles was also confirmed by solid-state ^{13}C CP-MAS NMR (Figure 2b). Resonances of the vinyl carbons at 122.9 and 136.7 ppm, of the methyl group (CH_3) attached to the vinyl group (C═C) at 22.0 ppm, and of the ester carbon ($-OCH_3$) at 166.0 ppm are clearly observed. The resonances at 66.0, 17.7, and 0.9 ppm are related to the propyl groups. A resonance at 8.4 ppm possibly comes from the carbon in the $Si(OCH_3)$ groups, indicating an incomplete hydrolysis of TMSPMA molecules, while a resonance at 59.0 ppm is perhaps due to residual ethanol solvent. These data further confirm the organic functionalization of the mesoporous silica particles.

Table 1. Chemical Shifts, Corresponding Relative Peak Areas Obtained by Curve Deconvolution, and Degree of Silica Condensation of the TMSPMA-Modified Mesoporous Silica Particles Obtained from ^{29}Si NMR[a,b]

	T^2	T^3	Q^3	Q^4
chemical shifts (ppm)	−59.4	−67.3	−101.9	−110.5
integrated peak area	7.8%	22.0%	34.1%	36.1%

[a] Total degree of silica condensation: 89.5%. [b] Q^3 and Q^4 represent silicon atoms (denoted as Si*) in $HOSi^*(OSi)_3$ and $Si^*(OSi)_4$ silicate species, respectively. T^2 and T^3 respectively represent the silicon atoms (denoted as Si*) in $R-Si^*(OH)(OSi)_2$ and $R-Si^*(OSi)_3$ species, where R is the non-hydrolyzable propyl methacrylate ligand.

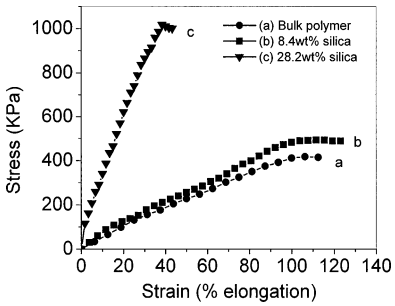

Figure 3. Tensile stress−strain curves of (a) pure poly(TMSPMA) and nanocomposites with (b) 8.4 wt % and (c) 28.2 wt % silica loading.

The solid-state ^{29}Si MAS NMR spectrum shown in Figure 2c provides information about the silicon environment and the degree of organic functionalization. Table 1 summarizes the chemical shifts and their deconvoluted peak areas. The Q^3 and Q^4 resonances at −101.9 and −110.5 ppm and T^2 and T^3 resonances at −59.4 and −67.3 ppm, respectively, are contributed from TEOS and (3-trimethoxysilyl)propyl methacrylate that form the hybrid silica networks. The presence of the T units ($T^2 + T^3$) further suggests the incorporation of propyl methacrylate ligands within the mesoporous silica particles. From Table 1, the molar percentage of the T units is around 30%, which is consistent with the molar percentage (30%) of (3-trimethoxysilyl)propyl methacrylate used in the synthesis process. The overall degree of silicon condensation calculated is around 89.5%.

2. Mechanical Properties. Figure 3 shows the representative stress−strain curves of the poly(TMSPMA)−silica nanocomposites, and the related mechanical properties are summarized in Table 2. Typically, curves 3a and 3b are exhibited by elastomers while curve 3c tends to be a tough plastic. Significant increases in the tensile strength and modulus relative to the bulk poly(TMSPMA) are observed. For example, approximately 20% and 142% increases in the tensile strength (480 and 993 vs 410 KPa) and 40% and 700% increases in the tensile moduli (526 and 2983 vs 378

(39) Brinker, C. J.; Scherer, G. W. *Sol−gel science: the physics and chemistry of sol−gel processing*; Academic Press: New York, 1990; pp 560−561.
(40) Wei, Y.; Yang, D.; Tang, L.; Hutchins, M. *J. Mater. Res.* **1993**, *8*, 1143−1152.
(41) Hergeth, W.-D.; Steinau, U. J.; Bittrich, H. J.; Schmutzler, K.; Wartewig, S. *Prog. Colloid Polym. Sci.* **1991**, *85*, 82−90.

Table 2. Mechanical Properties of the Bulk Polymer and Nanocomposites

samples	tensile strength at maximum (kPa)	strain at break (%)	tensile modulus (kPa)	toughness (kJ/m^3)
PTMSPMA	410	113	378 ± 37	290
PTMSPMA−8.4% silica	480	127	526 ± 16	322
PTMSPMA−28.2% silica	993	42	2983 ± 258	269

KPa) are observed for samples with 8.4 and 28.2 wt % silica, respectively. It should be mentioned that only previous studies on polymer−clay nanocomposites reported such a dramatic improvement in the tensile strength and modulus.[44,45] For instance, the reinforcement provided by clay at 16 wt % loading was manifested by more than a 10-fold improvement in both tensile strength and modulus. When compared with bulk polymers, the addition of reinforcing fillers such as fine and dense silica usually increases the tensile strength and moduli but decreases the strain at rupture.[6,9,43] We observed a similar decrease in the elongation at break from 113% (bulk polymer) to 42% with an increase of the silica loading to 28.2%. However, the 8.4% silica sample exhibited an increase of 14% over the bulk polymer in the elongation at break. The toughness of the polymer measured by the area under the stress−strain curve is a useful parameter[46] which quantifies the work expended in deforming the material. The last column in Table 2 lists the toughness derived from the stress−strain curves. As mentioned earlier, introducing dense filler particles usually improves the modulus but decreases the toughness. However, our results indicate that the nanocomposites exhibit improved or similar toughness compared with that of the bulk poly(TMSPMA) (322 and 269 kJ/m^3 vs 290 kJ/m^3). The above mechanical testing results suggest that mesoporous silica fillers may be suitable for both reinforcement and toughening of polymers. This possibly originates from the mesoporous structure of the filler particles. On one hand, the three-dimensional silica networks may provide a rigid inorganic framework to improve the mechanical strength and modulus, while on the other hand, the walls of mesoporous channels with a thickness of 0.5−2.0 nm may provide sites where the applied force or energy can be stored through the deformation of the silica framework, resulting in nanocomposites with better toughness. However, the mechanism of reinforcement and toughening is not clear at this stage, and it may also be related to an easier formation of cavitations in the system suggested by Lazzeri, Ayre, and Cheng et al.[47−49]

3. Confinement Effect. Figure 4 shows the DSC traces of poly(TMSPMA), the silica filler, and the nanocomposites. In the temperature interval of 100−200 °C shown in Figure 4d, the silica filler shows a strong endothermic peak, which may be caused by densification of the silica skeleton or by the removal of organic and solvent residues.[39] The bulk poly(TMPSMA) shows a readily observable glass transition at −9 °C. However, in the samples with 8.4 and 28.2 wt % silica, the glass transitions are not significantly observable (see Figure 4b and 4c), which may be attributed to the confined segmental motion of the molecular chains that are entrapped within the mesoporous channels.[7] As mentioned earlier, the pore surface of the mesoporous silica fillers have been modified with the monomer (TMSPMA) and may be copolymerized with the TMSPMA monomer. Thus, another reason is possibly related to the chemical bonding and strong interactions between the polymeric chains and the interior pore surface of the fillers. Undoubtedly, the strong interaction and chemical bonding can give rise to an increase in tensile strength and moduli compared with the flexible bulk polymer chains.

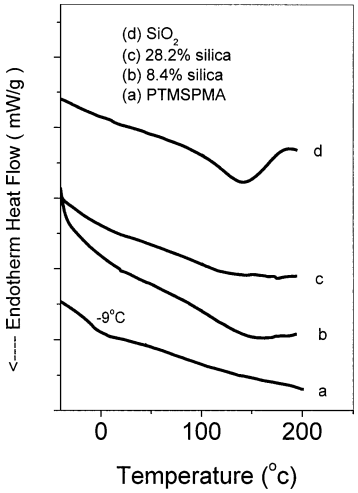

Figure 4. DSC traces of (a) poly(TMSPMA), (b) the nanocomposite with 8.4 wt % silica, (c) the nanocomposite with 28.2 wt % silica, and (d) silica filler particles.

4. Thermal Stability. The thermal stability of the nanocomposites has been studied using standard thermal analysis techniques. Figure 5 shows thermogravimetric analysis (TGA) curves of the pure poly(TMSPMA) (a), silica/poly(TMSPMA) nanocomposites with 8.4% silica loading (b), silica/poly(TMSPMA) nanocomposites with 28.2% silica loading (c), and the silica filler (d). As shown in Figure 5a, poly(TMSPMA) exhibits a two-step decomposition. The first decomposition occurs between 240 and 370 °C with an approximate weight loss of 75% due to the rapid thermal depolymerization of polyacrylates. The second decomposition stage centered at 400 °C with a further weight loss of 10% may be due to the continued decomposition of the polymer or the silica condensation reactions that occur between the organosilane $Si(OMe)_3$ groups. About 11.8% of silica is left remaining as residue at 700 °C. The TGA trace of the silica filler (trace d) shows a 20.8% weight loss between 200 and 450 °C, which may result from the decomposition of the TMSPMA molecules that were covalently bonded on the pore surface and from condensation reactions of surface silanols. The final residue at 700 °C approximates to 71.1% of the starting mass. On the basis of the above residue of pure poly(TMSPMA) and

(42) Wang, S.; Ahmad, Z.; Mark, J. E. *Chem. Mater.* **1994**, *6*, 943−946.
(43) Coltrain, B. K.; Landry, C. J. T.; O'Reilly, J. M.; Chamberlain, A. M.; Rakes, G. A.; Sedita, J. S.; Kelts, L. W.; Landry, M. R.; Long, V. K. *Chem. Mater.* **1993**, *5*, 1445−1455.
(44) Lan, T.; Pinnavaia, T. J. *Chem. Mater.* **1994**, *6*, 2216.
(45) Shi, H.; Lan, T.; Pinnavaia, T. J. *Chem. Mater.* **1996**, *8*, 1584.
(46) Sperling, L. H. *Introduction to physical polymer science*; John Wiley & Sons: New York, pp 399−400.
(47) Lazzeri, A.; Bucknall, C. B. *J. Mater. Sci.* **1993**, *28*, 6799−6808.
(48) Ayre, D. S.; Bucknall, C. B. *Polymer* **1998**, *39*, 4785−4791.
(49) Cheng, C.; Hiltner, A.; Baer, E.; Soskey, P. R.; Mylonakis, S. G. *J. Mater. Sci.* **1995**, *30*, 587−595.

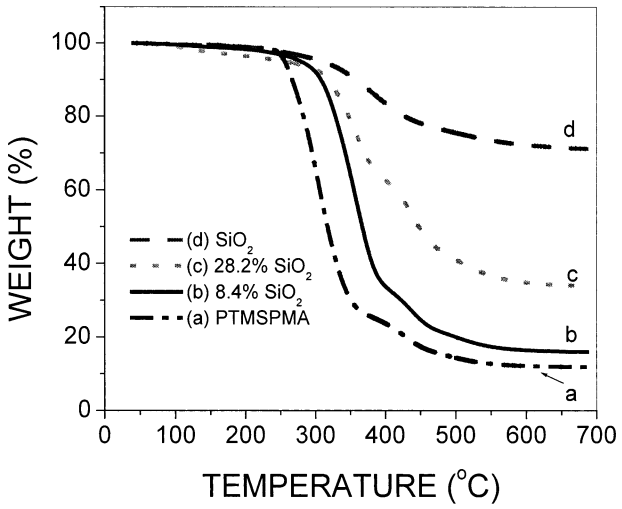

Figure 5. TGA curves of (a) poly(TMSPMA), (b) the nanocomposite with 8.4 wt % silica, (c) the nanocomposite with 28.2 wt % silica, and (d) silica filler particles.

Table 3. Calculated Residue Amounts and Experimental Residual Amount Based on TGA

samples	experimental (wt %)	calculated[a] (wt %)
PTMSPMA	11.8	
modified silica	71.1	
PTMSPMA−8.4% silica	16.0	16.8
PTMSPMA−28.2% silica	33.9	28.5

[a] Calculation was based on TGA data of both pure poly(TMSPMA) and modified silica.

modified silica fillers, the estimated residue amounts of silica/ploly(TMSPMA) nanocomposites after a TGA analysis are listed in Table 3. The TGA curves of the nanocomposites (trace b and trace c), fall between the pure polymer (trace a) and those of the fillers (trace d) with a three-stage decomposition. Increasing the filler content results in an increase of the first-step decomposition temperature. For example, the nanocomposite with 8.4% silica (trace b) shows a rapid weight loss of 56.5% from 250 to 380 °C, followed by a second weight loss of 20.4% between 380 and 450 °C, and a third weight loss of 4.0% from 450 to 700 °C. The composite with 28.2% silica (trace c) shows a relatively lower weight loss of about 28.6% at the first stage, a second weight loss of 25.5% from 350 to 450 °C, and a weight loss of 7.2% at the third stage. From the calculated and experimental results listed in Table 3, we found that the sample with 28.2% silica has a higher residue of 33.9% than the estimated result of 28.5%. However, the increase of silica loading improves the thermal stability, which is closely related to chemical bonding between the polymer chains and filler particles.

5. Morphology. Scanning electron microscopy (SEM) reveals the morphologies of the nanocomposites. Figure 6 shows SEM images of (a) the mesoporous silica particles, (b) and (c) the fracture surface of the bulk poly(TMSPMA) and the nanocomposites with 8.4% silica fillers, and (d) and (e) the fracture surfaces of the nanocomposites with 28.2% silica fillers. In Figure 6a, it can be seen that the sizes of the spherical silica particles range from 1 to 10 μm in diameter. Through SEM investigation, it is also observed that the fracture

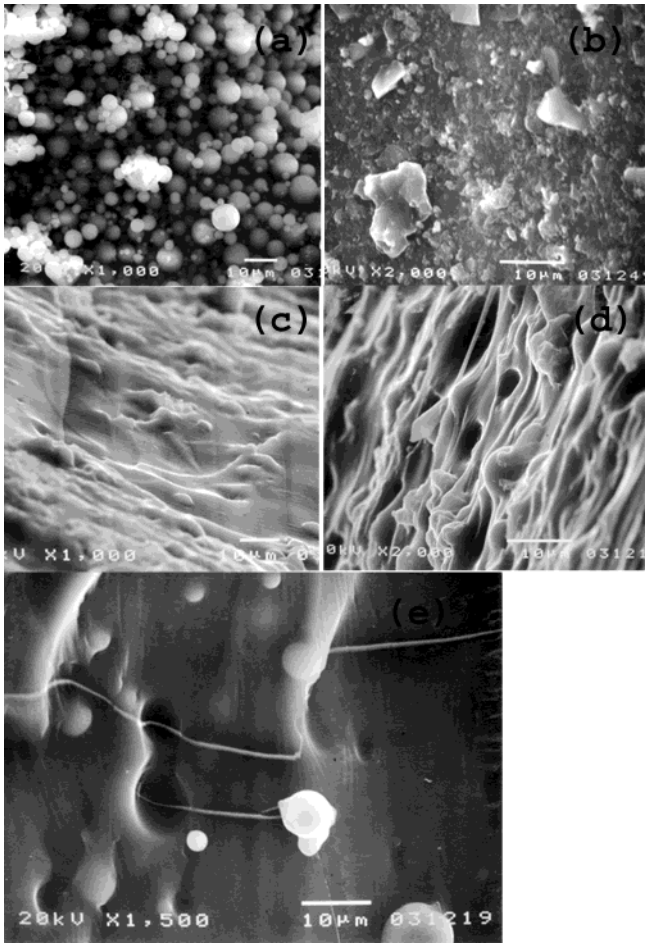

Figure 6. SEM images of (a) silica filler particles and fracture surface of (b) poly(TMSPMA), (c) the nanocomposite with 8.4 wt % silica, and (d,e) the nanocomposite with 28.2 wt % silica.

surface morphologies of the poly(TMSPMA) and the silica/poly(TMSPMA) nanocomposites are quiet different. The fracture surface of the nanocomposite shows a certain degree of chain orientation evidenced by the patterns of parallel lines seen in Figure 6c. It was found that the embedded filler particles also exhibited excellent interfacial bonding with the polymer in Figure 6d. Figure 6e shows that the voids left in the polymer matrix from the pulled out silica particles are connected with stranded polymer wires. Furthermore, it is observed that one polymer wire may connect a few silica particles. It appears that these polymer wires are composed of oriented polymer chain bundles. Infiltration and polymerization of the monomer within the pore channels form polymer chains that are confined within the mesoporous silica. Breaking of the nanocomposites in liquid nitrogen pulls and aligns these polymer chains, and they may further form the bundles shown in the Figure 6e. Thus, the SEM results suggest that as-synthesized nanocomposites are composed of polymer that threads through the mesoporous silica particles and the polymer formed among these filler particles. Compared with conventional particle/polymer composites prepared using dense particle as fillers, these porous fillers may serve as pseudo-cross-linking points within the nanocomposites and contribute to the improved mechanical properties.

Conclusions

The organic-modified mesoporous silica particles have been synthesized through hydrolysis and condensation of TMSPMA with TEOS and co-assembly of the silicate species with surfactant followed by selective removal of surfactant. The resulting silica particles exhibit the wormlike pore structure as indicated by TEM study. FTIR and NMR results suggest that the organic moieties are linked covalently to the mesoporous silica framework. These organic-modified particles were used as fillers to synthesize poly(TMSPMA)/silica nanocomposites with different silica loadings using infiltration and in situ polymerization techniques. DSC traces show an undetectable glass transition temperature with silica content of 8.4 and 28.2 wt % due to a possible confinement effect or a strong chemical bonding and strong filler/polymer interactions. Thermal analysis studies indicate that an increase in silica loading improves the thermal stability of nanocomposites. The mechanical testing results suggest that the use of mesoporous silica particles as fillers may significantly improve the tensile strength, modulus, and toughness of the nanocomposites with little sacrifice on the strain at break. We consider that the chemical bonding and strong interactions between the polymer and the filler, confined segmental motion of the polymer chains within the mesoporous channels, and the use of the silica particles as pseudo-cross-linking points may contribute to the improved mechanical properties.

Acknowledgment. The authors gratefully acknowledge support of this work by NASA, the National Science Foundation, Sandia National Laboratories, and the Advanced Materials Research Institute at the University of New Orleans through DARPA Grant No. MDA972-97-1-0003 and through the Louisiana Board of Regents Contract No. NSF/LEQSF(2001-04)-RII-03. We thank Dr. Weilie Zhou for assisting with the SEM measurements.

Supporting Information Available: Discussion on conversion of monomre and figure of FT-IR spectra (PDF). This material is available free of charge via the Internet at http://pubs.acs.org.

CM0300866